Article
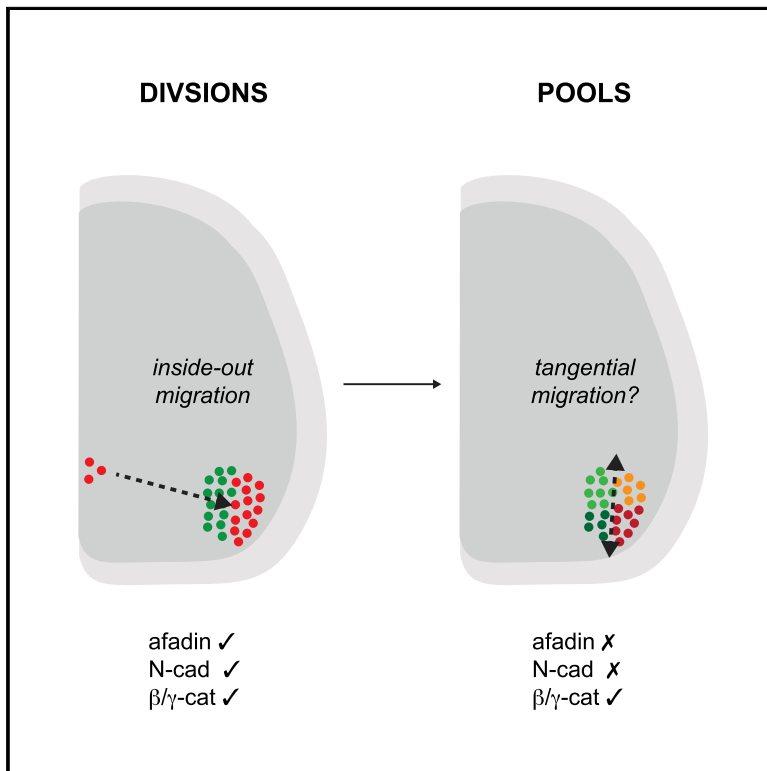
Nuclear Organization in the Spinal Cord Depends on Motor Neuron Lamination Orchestrated by Catenin and Afadin Function

Graphical Abstract

Authors

Carola Dewitz, Sofia Pimpinella,
Patrick Hackel, Altuna Akalin,
Thomas M. Jessell, Niccolò Zampieri

Correspondence

niccolo.zampieri@mdc-berlin.de

In Brief

The developmental mechanisms controlling the ordered grouping of neurons into nuclei are still not clear. Dewitz et al. show that nuclear organization of motor neurons into pools relies on coordinated afadin and N-cadherin/catenin function orchestrating a two-step process that controls precise motor neuron positioning in the spinal cord.

Highlights

- Inside-out migration is the initial step of motor neuron positioning

- Coordinated afadin and catenin signaling orchestrates motor pool organization

- Afadin is required for motor neuron inside-out migration and layering of divisions

CellPress

Nuclear Organization in the Spinal Cord Depends on Motor Neuron Lamination Orchestrated by Catenin and Afadin Function

Carola Dewitz,[1,2,9] Sofia Pimpinella,[1,2,9] Patrick Hackel,[1,2] Altuna Akalin,[2,3] Thomas M. Jessell,[4,5,6,7,8] and Niccolò Zampieri[1,2,10,*]
[1]Max Delbrück Center for Molecular Medicine in the Helmholtz Association (MDC), 13125 Berlin, Germany
[2]Cluster of Excellence NeuroCure, Neuroscience Research Center, Charité Universitätsmedizin Berlin, Charitéplatz 1, 10117 Berlin, Germany
[3]Berlin Institute for Medical Systems Biology, 13125 Berlin, Germany
[4]Department of Neuroscience
[5]Department of Biochemistry
[6]Department of Molecular Biophysics
[7]Howard Hughes Medical Institute
[8]Kavli Institute for Brain Science
Columbia University, New York, NY 10032, USA
[9]These authors contributed equally
[10]Lead Contact
*Correspondence: niccolo.zampieri@mdc-berlin.de
https://doi.org/10.1016/j.celrep.2018.01.059

SUMMARY

Motor neurons in the spinal cord are found grouped in nuclear structures termed pools, whose position is precisely orchestrated during development. Despite the emerging role of pool organization in the assembly of spinal circuits, little is known about the morphogenetic programs underlying the patterning of motor neuron subtypes. We applied three-dimensional analysis of motor neuron position to reveal the roles and contributions of cell adhesive function by inactivating N-cadherin, catenin, and afadin signaling. Our findings reveal that nuclear organization of motor neurons is dependent on inside-out positioning, orchestrated by N-cadherin, catenin, and afadin activities, controlling cell body layering on the medio-lateral axis. In addition to this lamination-like program, motor neurons undergo a secondary, independent phase of organization. This process results in segregation of motor neurons along the dorso-ventral axis of the spinal cord, does not require N-cadherin or afadin activity, and can proceed even when medio-lateral positioning is perturbed.

INTRODUCTION

The precise spatial organization of neuronal cell bodies in the nervous system is an important determinant of identity, connectivity, and function (Leone et al., 2008; Sürmeli et al., 2011; Bikoff et al., 2016; Oishi et al., 2016). In the central nervous system (CNS), neurons are broadly arranged following two main anatomical plans that involve laminar and nuclear organization (Ramon y Cajal, 1894). Distinct neuronal subtypes are often found in stereotyped positions that are predictive of their input-output connectivity patterns. Defining the mechanisms governing the positional organization of neurons is an important step for understanding the developmental processes responsible for the assembly and function of neural circuits. The cellular and molecular underpinnings of neuronal positioning have been mostly studied in the developing cortex, where signaling pathways controlling lamination and ordered distribution of neuronal populations have been identified (Rakic, 1974; Hatten, 1999; Bielas and Gleeson, 2004; Marín et al., 2010). By comparison, less is known about the developmental programs used in the generation of neuronal nuclei of appropriate location, size, and cell type composition.

A striking example of nuclear organization in the CNS is apparent in the positioning of limb-innervating motor neurons in the lateral motor column (LMC) of the spinal cord. LMC neurons are found clustered into discrete structures termed motor pools, which occupy stereotyped positions in the ventral spinal cord (Romanes, 1964; Vanderhorst and Holstege, 1997). Each motor pool consists of a functionally coherent subset of motor neurons whose location is linked to the position and identity of its muscle target in the limb (McHanwell and Biscoe, 1981; Dasen and Jessell, 2009). The genesis of motor pools is believed to involve processes that reflect the hierarchical organization of LMC neurons, first in medial (m) and lateral (l) divisions and, ultimately, into motor pools (Landmesser, 2001). First, LMCm neurons are generated from the motor neuron progenitor zone. Then, later-born LMCl neurons migrate through LMCm neurons to reach their final settling position in the lateral ventral horn (Hollyday and Hamburger, 1977; Sockanathan and Jessell, 1998). Last, defined subsets of motor neurons within each division coalesce to form motor pools (Lin et al., 1998). The precise molecular and cellular programs coordinating the ordered migration of motor neurons to the ventral horn and their sorting into motor pools are not yet understood.

To date, the main cell-surface molecules that have been shown to be involved in motor neuron positional organization are members of the classical cadherin family of adhesion molecules (Price et al., 2002; Demireva et al., 2011; Bello et al., 2012; Astick et al., 2014). Type II cadherin combinatorial expression defines motor pools at a molecular level, and manipulation of cadherin profiles in chick embryos disrupts motor neuron organization (Price et al., 2002). In mouse embryos, inactivation of N-cadherin, a type I cadherin expressed by all motor neurons, as well as perturbation of all classical cadherin function through β- and γ-catenin elimination, have been shown to prevent divisional segregation and pool clustering (Demireva et al., 2011). However, the contributions of type I and type II cadherins and the nature of the morphogenetic events that lead to motor pool formation are not clear. In addition, it cannot be excluded that other signaling pathways might conspire with cadherins in the control of motor neuron organization. Catenin adhesive signaling has been shown to cooperate with nectins, a family of Ca^{2+}-independent adhesion molecules of the immunoglobulin superfamily, via direct interaction with afadin (Mandai et al., 1997; Takai and Nakanishi, 2003; Takai et al., 2008; Harris and Tepass, 2010). Afadin is a cytosolic adaptor protein that controls nectin adhesive function in similar ways as catenins regulate cadherin activity. Cross-talk between nectin/afadin and cadherin/catenin signaling is believed to be an important regulator of cell adhesive function (Takai and Nakanishi, 2003). In the developing brain, genetic elimination of afadin has been shown to impair synapse formation and neuronal migration (Beaudoin et al., 2012; Gil-Sanz et al., 2014; Yamamoto et al., 2013; Miyata et al., 2017). A potential role for nectin/afadin signaling in motor neuron organization in the spinal cord has not been explored.

In this study, we established quantitative three-dimensional analysis of motor neuron position to investigate the roles and contributions of cell adhesive signaling in nuclear organization in the spinal cord. Our analysis reveals that β- and γ-catenin activity has a dual effect; along the medio-lateral axis, it selectively controls LMCl neuronal inside-out migration, and along the dorso-ventral axis, it controls columnar positioning as well as the segregation of motor pools. We find that N-cadherin is required for mediating LMCl neuronal migration and overall columnar location but is dispensable for segregation of motor neurons into pools on the dorso-ventral axis. We also identify afadin as an important player in the control of motor neuron organization, selectively acting on the positioning of LMCl neurons. Together, these findings support a model where motor neuron nuclear organization is developmentally orchestrated using a two-step process: first, an N-cadherin/catenin/afadin-dependent radial phase that results in divisional lamination by controlling LMCl neuron position and a second, independent phase that promotes clustering of motor pools along the dorso-ventral axis.

RESULTS

Previous studies analyzing motor neuron organization used methods aimed at quantifying the intermixing of different neuronal subtypes at a local level in the ventral horn, thus losing information regarding possible changes in overall motor neuron position in the spinal cord (Price et al., 2002; Demireva et al.,

2011). To reveal the cellular and molecular mechanisms controlling motor pool formation, we elected to analyze motor neuron position in the spinal cord in three dimensions (Stepien et al., 2010; Bikoff et al., 2016).

We acquired images of consecutive transverse spinal cord sections from rostral lumbar levels and assigned Cartesian coordinates to each motor neuron subtype identified using specific transcription factor expression profiles (for details, see Supplemental Experimental Procedures). To validate this approach, we analyzed LMC divisional organization in embryonic day 13.5 (E13.5) mouse embryos and plotted transverse and longitudinal projections of cell body position coordinates to visualize motor neuron distributions on the medio-lateral, dorso-ventral, and rostro-caudal axes for three biological replicates (Figures 1 and S1). Medial and lateral LMC neurons were always positioned in the same area of the ventral horn, segregated from each other, as expected by stereotyped positioning of motor neuron divisional subtypes (Figures 1A–1C; Romanes, 1964; Vanderhorst and Holstege, 1997). Accordingly, the average settling positions of LMCm and LMCl neurons were conserved across individuals (Figure 1D). Distribution analysis confirmed that LMCm and LMCl neuron positions were reproducible (Figures 1E and 1F and data not shown).

Finally, we tested the variability in motor neuron subtype position by comparing datasets from different embryos using correlation analysis. We found that only datasets of motor neurons sharing the same subtype identity were highly correlated with each other (LMCm versus LMCm and LMCl versus LMCl, r ≥ 0.9; Figure 1G), whereas datasets belonging to motor neurons with different divisional identity were poorly correlated (LMCm versus LMCl and LMCl versus LMCm, r ≤ 0.3; Figure 1G). Thus, these experiments show that analysis of cell body position coordinates is a reproducible method to precisely assess motor neuron spatial organization in the embryonic spinal cord.

β- and γ-Catenin Inactivation Impairs LMCl Medio-lateral Positioning

Previous work, although clearly pointing to an important role for N-cadherin and β- and γ-catenin signaling in motor neuron organization, did not provide insights into their specific roles or the precise nature of the positioning defects (Demireva et al., 2011). Thus, we decided to apply three-dimensional positional analysis to β- and γ-catenin mutant embryos and eliminated catenins from motor neurons by crossing *olig2::Cre* mice with conditional β- and γ-catenin alleles ($\beta\gamma^{\Delta MN}$; Demireva et al., 2011).

First, we focused on motor neuron divisions and generated datasets of cell body position coordinates for LMCm and LMCl neurons. Transverse and longitudinal contour plots from control and $\beta\gamma^{\Delta MN}$ embryos revealed clear differences in medio-lateral and dorso-ventral divisional organization (Figures 2A–2F). In $\beta\gamma^{\Delta MN}$ embryos, we observed an overlap in the distribution of LMCm and LMCl neurons on the medio-lateral axis (Figures 2E–2H). Surprisingly, the medio-lateral distribution and average position of LMCm neurons in control and $\beta\gamma^{\Delta MN}$ embryos was not significantly different, whereas $\beta\gamma^{\Delta MN}$ LMCl neurons were found in medial positions, causing intermixing with LMCm neurons (Figures 2I and S2A). On the dorso-ventral axis, we observed a ventral shift in the location of both LMCm and LMCl neurons (Figures 2J–2L).
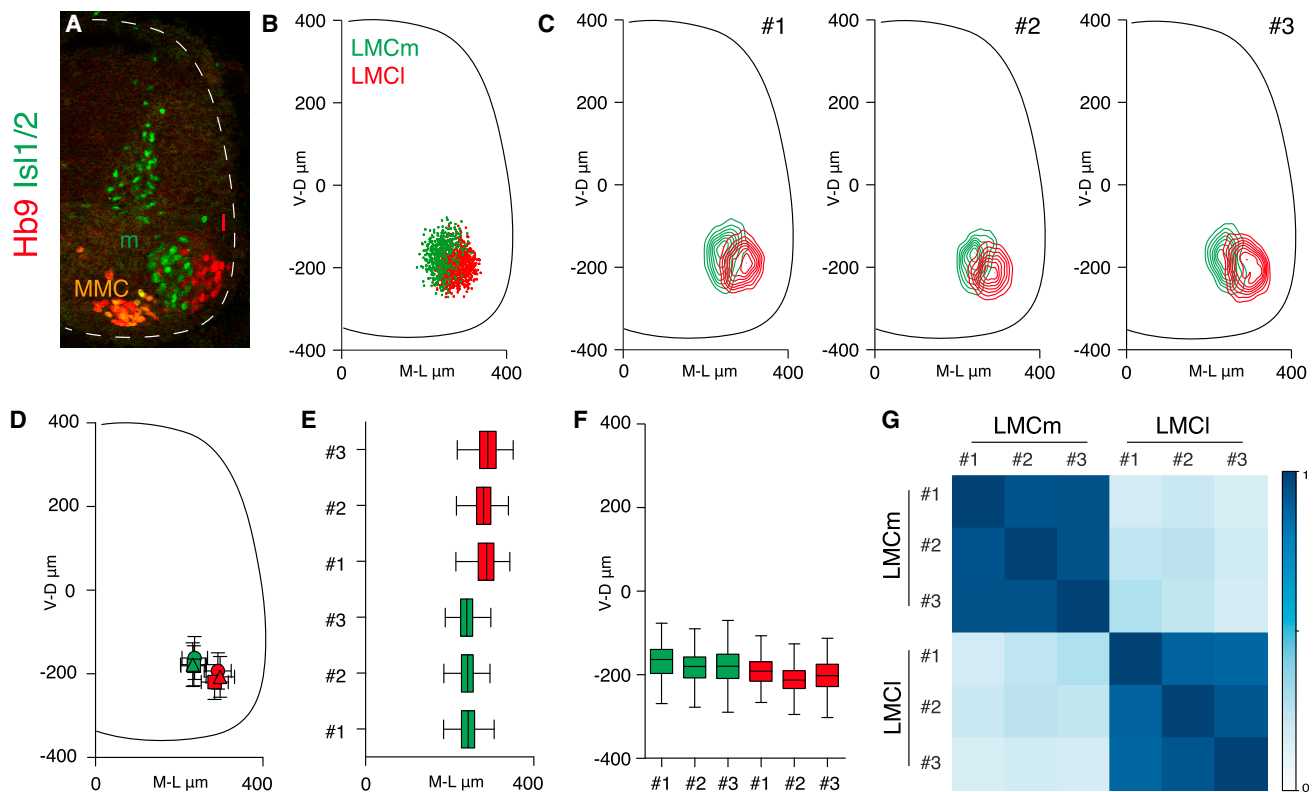
Figure 1. Three-Dimensional Analysis of Motor Neuron Positions in the Developing Spinal Cord
(A) Motor neuron organization in an E13.5 control embryo at lumbar spinal level. Isl1/2$^+$, LMCm neurons; Hb9$^+$, LMCl neurons; Isl1/2$^+$, Hb9$^+$, MMC neurons.
(B) Digitally reconstructed distribution of LMC neurons at L1–L3, shown as a transverse projection.
(C) Transverse contour density plots of LMCm (green) and LMCl (red) neurons.
(D) Medio-lateral and dorso-ventral positions (mean position ± SD) of LMCm (green) and LMCl (red) neurons (#1, ○; #2, □; #3, △).
(E and F) Boxplots showing distributions of LMCm (green) and LMCl (red) neurons along medio-lateral (E) and dorso-ventral (F) axes.
(G) Correlation analysis of LMC positional coordinates. The scale bar indicates correlation values.
For additional data examining LMC rostro-caudal positions, see Figure S1.

We did not detect any local variation in the rostro-caudal distribution of motor neurons, with LMCl neurons from $\beta\gamma^{\Delta MN}$ embryos consistently being found in the medial position at all levels analyzed (Figures 2E and 2F). To provide an overall assessment of divisional organization in catenin mutants, we used correlation analysis. LMCl neuron positions of $\beta\gamma^{\Delta MN}$ and control embryos were no longer correlated ($\beta\gamma^{\Delta MN}$ versus control LMCl, r < 0.1; Figure 2M). In contrast, LMCm neuron positions were still partially correlated despite the ventral shift of the whole motor column in $\beta\gamma^{\Delta MN}$ mutant embryos ($\beta\gamma^{\Delta MN}$ versus control LMCm, r = 0.58; Figure 2M). Accordingly, datasets from LMCm neurons of $\beta\gamma^{\Delta MN}$ and control embryos were still highly correlated when only medio-lateral coordinates were considered ($\beta\gamma^{\Delta MN}$ versus control LMCm, r > 0.9, $\beta\gamma^{\Delta MN}$ versus control LMCl, r < 0.3; Figure S2B).

Thus, three-dimensional analysis uncovers that elimination of β- and γ-catenin function disrupts divisional organization in two ways: on the medio-lateral axis by preventing lateral positioning of LMCl neurons and on the dorso-ventral axis by shifting ventrally the location of the whole column (Figure 2N).

β- and γ-Catenin Inactivation Perturbs Medio-lateral and Dorso-ventral Pool Organization
To examine how β- and γ-catenin signaling affects motor neuron subtype position within divisions, we next studied the organization of motor pools (Figures 3A and 3B). We first assessed the effect of β- and γ-catenin inactivation on the positioning of pools that normally reside in different LMC divisions by analyzing the medio-lateral segregation of medial (hamstring, H) from lateral pools (rectus femoris/tensor fasciae latae, R/T; De Marco Garcia and Jessell, 2008).

In control embryos, H neurons were found clearly separated from R/T neurons, respectively, in medial and lateral positions (Figures 3C and 3E). In $\beta\gamma^{\Delta MN}$ embryos, H and R/T pools were no longer segregated and occupied largely overlapping areas (Figures 3D and 3F). Distribution and average positional analyses on the medio-lateral axis showed that, consistent with the LMCl phenotype, lateral R/T neurons were found in medial position (Figures 3G–3I). We next assessed the dorso-ventral organization of motor neurons by analyzing the segregation of dorsal (vasti, V) from ventral pools (H and R/T). Contour, density, and average position analyses showed
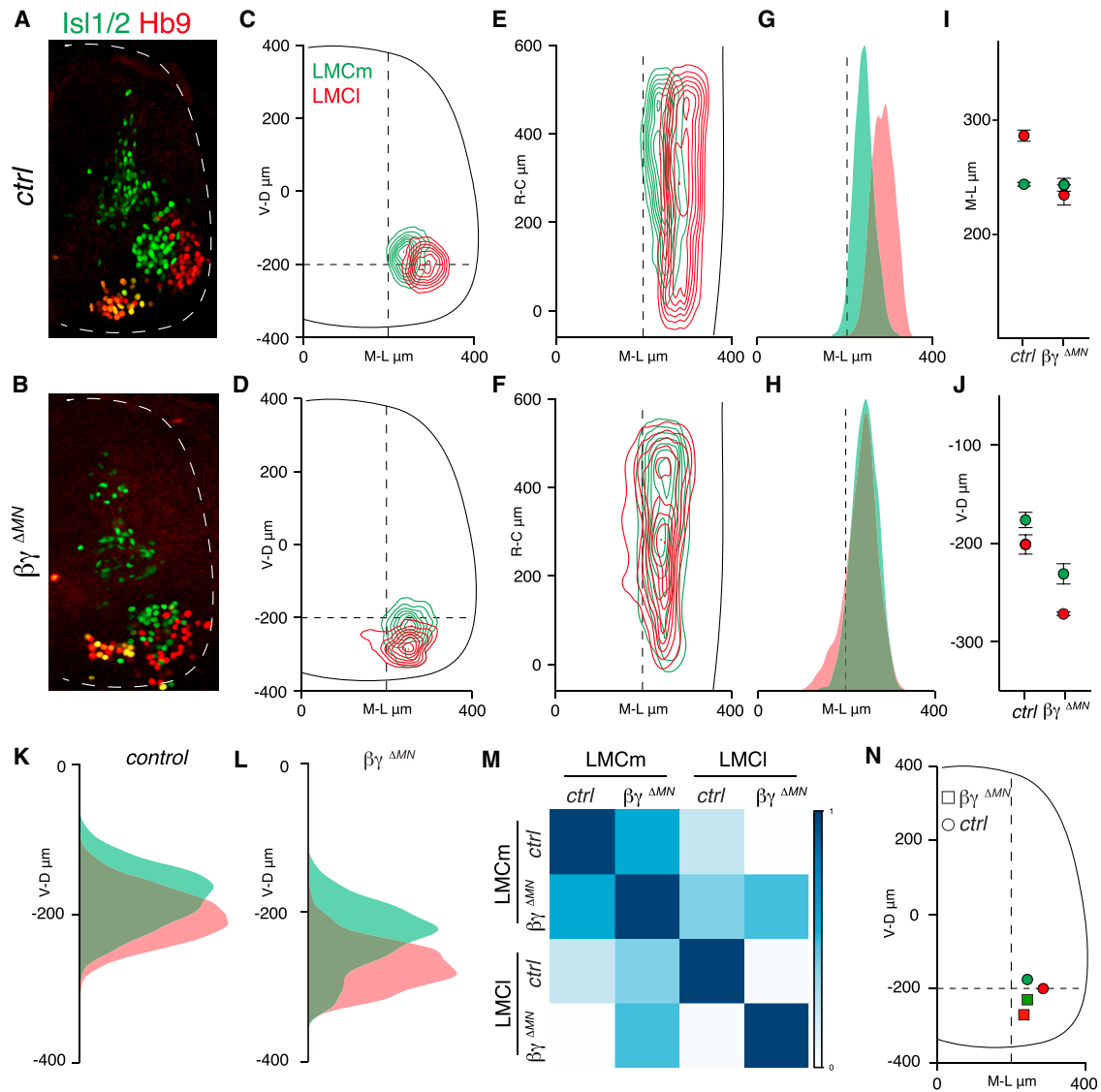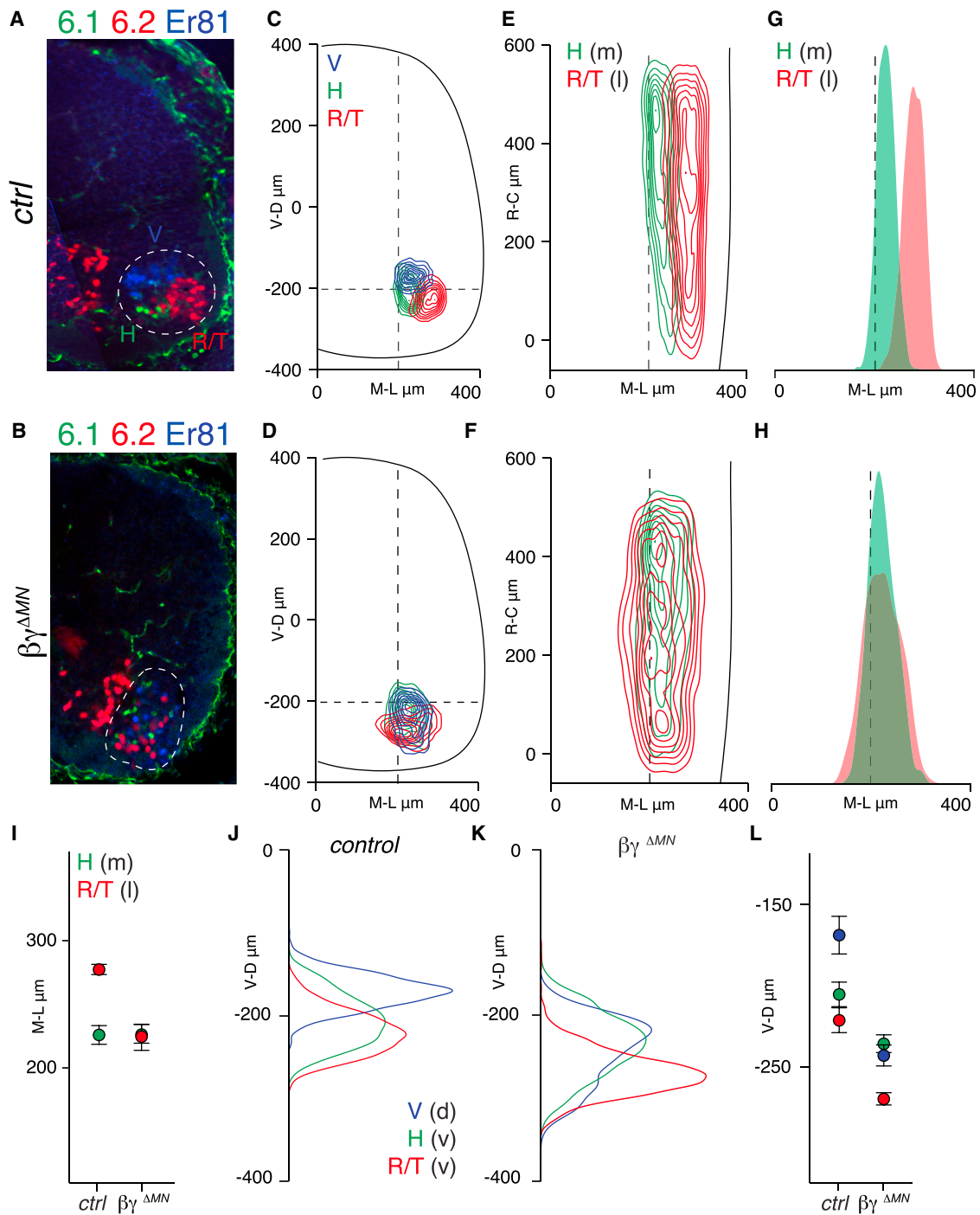
Figure 2. Catenin Inactivation Perturbs Medio-lateral and Dorso-ventral Motor Neuron Organization

(A and B) Organization of Isl1/2$^+$ medial and Hb9$^+$ lateral LMC neurons at lumbar spinal levels in E13.5 control (A) and $\beta\gamma^{\Delta MN}$ (B) embryos.

(C and D) Transverse contour density plots of LMCm (green) and LMCl (red) neurons in control (C) and $\beta\gamma^{\Delta MN}$ (D) embryos.

(E and F) Longitudinal contour density plots of LMCm (green) and LMCl (red) neurons in control (E) and $\beta\gamma^{\Delta MN}$ (F) embryos.

(G and H) Medio-lateral density plots of LMCm (green) and LMCl (red) neurons in control (G) and $\beta\gamma^{\Delta MN}$ (H) embryos.

(I) Average medio-lateral position of LMCm (green) and LMCl (red) neurons in control and $\beta\gamma^{\Delta MN}$ embryos (mean ± SD; differences significant for LMCl neurons; t test, p < 0.001).

(J) Average dorso-ventral position of LMCm (green) and LMCl (red) neurons in control and $\beta\gamma^{\Delta MN}$ embryos (mean ± SD; differences significant for LMCm and LMCl neurons; t test: LMCm, p < 0.01; LMCl, p < 0.001).

(K and L) Dorso-ventral density plots of LMCm (green) and LMCl (red) neurons in control (K) and $\beta\gamma^{\Delta MN}$ (L) embryos.

(M) Correlation analysis of LMC neuron positional coordinates in control and $\beta\gamma^{\Delta MN}$ embryos. The scale bar indicates correlation values.

(N) Average medio-lateral and dorso-ventral positions of LMCm (green) and LMCl (red) neurons in control and $\beta\gamma^{\Delta MN}$ embryos (mean).

For additional data regarding LMC organization in $\beta\gamma^{\Delta MN}$ embryos, see Figure S2.

that segregation of pools on the dorso-ventral axis is lost in $\beta\gamma^{\Delta MN}$ embryos (Figures 3J–3L and S2C–S2F). Thus, the data indicate that β- and γ-catenin inactivation disrupts motor pool segregation both on the medio-lateral and the dorso-ventral axes.

N-Cadherin Does Not Affect Dorso-ventral Pool Segregation

Previous motor neuron mixing analysis suggested that the defects of N-cadherin mutants phenocopied the ones observed in β- and γ-catenin mutants, albeit less severely (Demireva et al.,

Figure 3. Catenin Inactivation Disrupts Medio-lateral and Dorso-ventral Pool Segregation

(A and B) Organization of H (Nkx6.1[+]), R/T (Nkx6.2[+]), and V (Er81^{+}) motor pools in E13.5 control (A) and $\beta\gamma^{\Delta MN}$ (B) embryos. The motor neuron area is delimited by a dashed line.

(C and D) Transverse contour density plots of H (green), R/T (red), and V (blue) motor pools in control (C) and $\beta\gamma^{\Delta MN}$ (D) embryos.

(E and F) Longitudinal contour density plots of H (green, medial) and R/T (red, lateral) neurons in control (E) and $\beta\gamma^{\Delta MN}$ (F) embryos.

(G and H) Medio-lateral density plots of H (green, medial) and R/T (red, lateral) neurons in control (G) and $\beta\gamma^{\Delta MN}$ (H) embryos.

(I) Average medio-lateral position of H (green, medial) and R/T (red, lateral) neurons in control and $\beta\gamma^{\Delta MN}$ embryos (mean ± SD; differences significant for H neurons; t test, $p < 0.01$).

(legend continued on next page)

2011). We next asked whether N-cadherin elimination recapitulates the β- and γ-catenin inactivation phenotypes using the three-dimensional position assay. Thus, we eliminated N-cadherin from motor neurons by crossing an *olig2::Cre* driver line with mice carrying floxed N-cadherin alleles ($N^{\Delta MN}$; Demireva et al., 2011).

The analysis revealed defects in the positioning of LMC neurons in $N^{\Delta MN}$ embryos (Figures 4A–4C). Divisional distribution on the medio-lateral axis showed that elimination of N-cadherin selectively impairs lateral positioning of LMCl neurons (Figures 4D and S5A and S5B). On the dorso-ventral axis, all LMC neurons in $N^{\Delta MN}$ embryos were found in more ventral positions (Figures 4E and S5C and S5E). However, although the medio-lateral defect in $N^{\Delta MN}$ embryos only partially recapitulates the one observed in $\beta\gamma^{\Delta MN}$ embryos, the dorso-ventral phenotype is nearly indistinguishable (Figures 4D and 4E).

We next looked at motor pool organization (Figures 4F and 4G). Analysis of medio-lateral distribution of medial (H) and lateral (R/T) pools confirmed that elimination of N-cadherin specifically impairs LMCl neuron subtype positioning (Figures S3A–S3H). Surprisingly, on the dorso-ventral axis, transverse contour analysis indicated that, despite the ventral shift in columnar location, motor pool segregation in the absence of N-cadherin function was not completely eroded, as observed in $\beta\gamma^{\Delta MN}$ embryos (Figures 4F and 4G and 3B and 3D). Density and average position analyses on the dorso-ventral axis confirmed that segregation of motor pool subtypes was mostly preserved (Figures 4I and 4J). As a consequence, the average distance between dorsal and ventral pools in $N^{\Delta MN}$ embryos was not significantly different from control embryos, as opposed to $\beta\gamma^{\Delta MN}$ embryos (Figure 4H). Thus, three-dimensional positional analysis reveals that N-cadherin elimination, although accounting entirely for the columnar positioning defect and partially for the LMCl medio-lateral phenotype, does not recapitulate the dorso-ventral motor pool mixing phenotype of β- and γ-catenin mutants.

Motor Neuron Generation, Differentiation, and Columnar Organization in Afadin Mutant Embryos

The limited effect on dorso-ventral pool segregation observed after N-cadherin elimination suggests the involvement of additional catenin-dependent effectors. Type II cadherins are obvious candidates because motor neuron subtypes can be distinguished by their combinatorial expression, and manipulations that equalize type II cadherin profiles disrupt motor pool segregation in chick spinal cord (Price et al., 2002). However, genetic mouse models where type II cadherins have been eliminated either individually or in combination exhibit no defect in motor neuron positioning (C.D. and N.Z., unpublished data). Thus, we next asked whether catenins might regulate dorso-ventral motor neuron sorting by engaging the activity of nectins. To start studying a possible involvement of nectin signaling, we decided to focus on afadin, an intracellular transducer molecule

that is necessary for nectin-mediated adhesive function (Takai and Nakanishi, 2003).

Afadin mRNA and protein are expressed in motor neurons throughout the developmental period encompassing their generation, migration, and final positioning in the ventral horn of the spinal cord (Figures 5A and 5B and S4A and S4B). Because afadin constitutive inactivation results in gross developmental defects and abortion by E10.5 because of its essential roles during gastrulation, we targeted afadin deletion to motor neurons by using a conditional approach (Ikeda et al., 1999). Afadin heterozygous mutants are indistinguishable from wild-type mice; thus, we crossed mice carrying one copy of a constitutive mutant allele (*afadin*⁻) and one copy of a floxed allele (*afadin*^fl) with the *olig2::Cre* driver line to restrict recombination to motor neuron progenitors and generated *afadin*^ΔMN mice (*afadin*^fl/−; *olig2::Cre*^+/−; Beaudoin et al., 2012; Dessaud et al., 2007).

We found that afadin was effectively eliminated from spinal motor neurons in *afadin*^ΔMN embryos (Figures 5C–5F). We first evaluated whether afadin elimination has an effect on motor neuron generation and subtype identity. Motor neuron columnar subtypes were distinguished using transcription factor expression profiles (Dasen et al., 2008). The total number of neurons generated was similar in control and *afadin*^ΔMN embryos, and we did not observe significant differences in the numbers of LMC and MMC neurons (Figures 5G–5I). Similarly, we did not detect any differences in the generation, differentiation, and overall organization of motor columns at thoracic levels (Figures 5J–5L and data not shown).

Afadin Function Is Required for Motor Neuron Divisional and Pool Organization

Next we assessed whether divisional and pool organization is affected by the loss of afadin. In E13.5 *afadin*^ΔMN embryos, we detected intermixing of medial and lateral LMC neurons as well as defects in the clustering and segregation of motor pools (Figures 6A–6D and 6F–6I). However, we observed no changes in the numbers of motor neurons allocated to the lateral and medial division or to the pool subtypes analyzed (Figures 6E and 6J). Thus, afadin elimination does not interfere with the acquisition of motor neuron divisional and pool identities but selectively abolishes their positional organization.
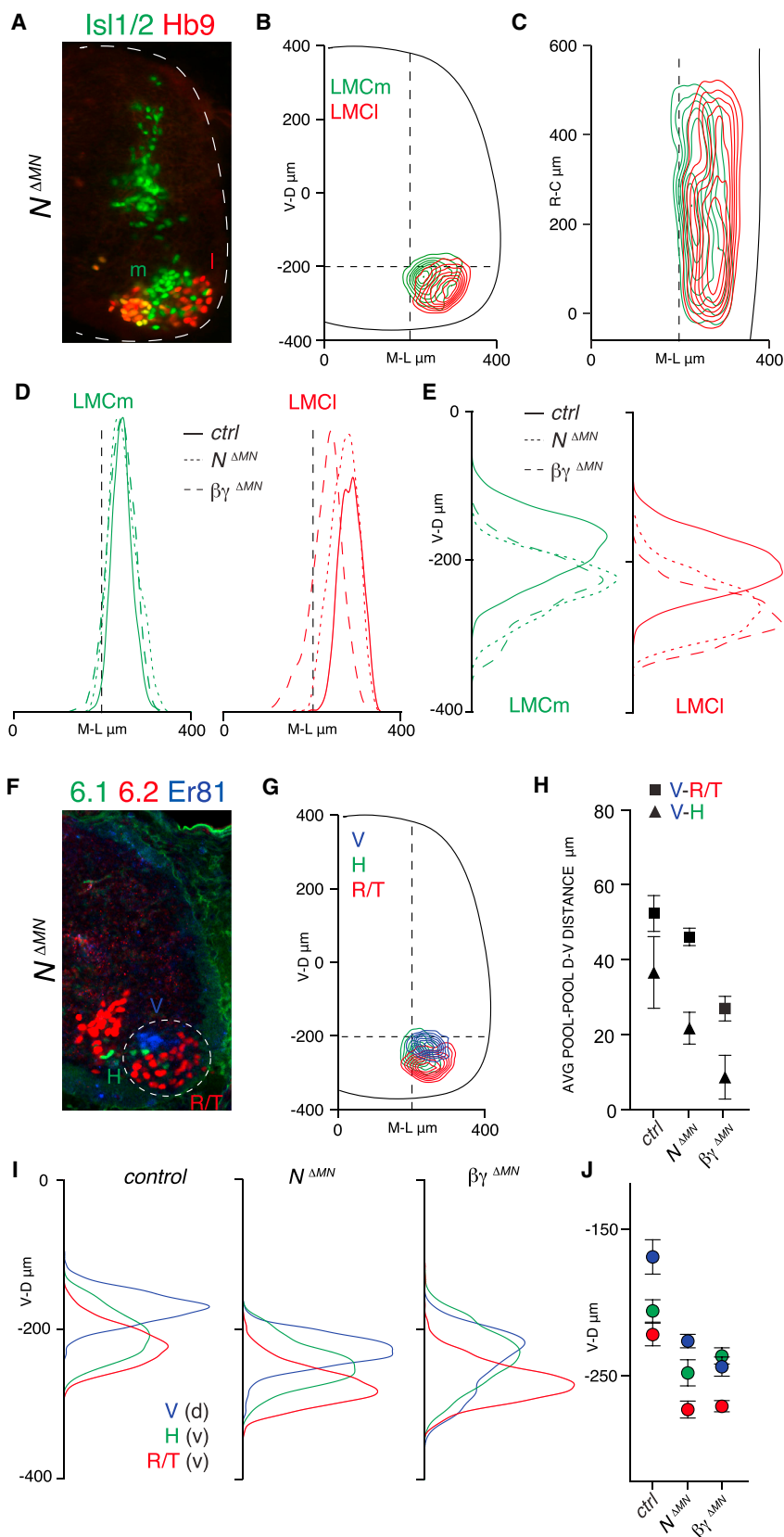
Afadin Elimination Selectively Impairs LMCl Neuron Positioning

We then used three-dimensional position analysis to assess motor neuron organization defects in *afadin*^ΔMN embryos in more detail. At a divisional level, we observed a perturbation in the segregation of LMCm and LMCl neurons (Figures 7A and 7B). Medio-lateral distribution and average position analyses indicated that afadin inactivation selectively impairs the ability of LMCl neurons to settle laterally to LMCm neurons (Figures 7C and 7D and S5A and S5B). On the dorso-ventral axis, we

---

(J and K) Dorso-ventral density plots of H (green, ventral), R/T (red, ventral), and V (blue, dorsal) neurons in control (J) and $\beta\gamma^{\Delta MN}$ (K) embryos.

(L) Average dorso-ventral position of H (green), R/T (red), and V (blue) neurons in control and $\beta\gamma^{\Delta MN}$ embryos (mean ± SD; differences significant for H, R/T, and V neurons; t test: H, $p < 0.05$; R/T and V, $p < 0.001$).

For additional data regarding pool organization in $\beta\gamma^{\Delta MN}$ embryos, see Figure S2.

A Isl1/2 Hb9

B

C

D LMCm LMCl

E

F 6.1 6.2 Er81

G

H

I control $N^{\Delta MN}$ $\beta\gamma^{\Delta MN}$

J

Figure 4. N-Cadherin Elimination Does Not Interfere with Dorso-ventral Pool Segregation

(A) Organization of Isl1/2$^+$ medial and Hb9$^+$ lateral LMC neurons at lumbar spinal levels in E13.5 $N^{\Delta MN}$ embryos.

(B and C) Transverse (B) and longitudinal (C) contour density plots of LMCm (green) and LMCl (red) neurons in $N^{\Delta MN}$ embryos.

(D) Medio-lateral density plots of LMCm (green) and LMCl (red) neurons in control (solid line), $N^{\Delta MN}$ (dashed line), and $\beta\gamma^{\Delta MN}$ (dotted line) embryos.

(E) Dorso-ventral density plots of LMCm (green) and LMCl (red) neurons in control (solid line), $N^{\Delta MN}$ (dashed line), and $\beta\gamma^{\Delta MN}$ (dotted line) embryos.

(F) Organization of H (Nkx6.1$^+$), R/T (Nkx6.2$^+$), and V (Er81$^+$) motor pools in $N^{\Delta MN}$ embryos. The motor neuron area is delimited by a dashed line.

(G) Transverse contour density plots of H (green), R/T (red), and V (blue) motor pools in $N^{\Delta MN}$ embryos.

(H) Average distance between dorso-ventral positions of V-R/T (■) and V-H (▲) pools in control, $N^{\Delta MN}$, and $\beta\gamma^{\Delta MN}$ embryos (mean ± SD; differences significant for V-R/T p < 0.001: control versus $\beta\gamma^{\Delta MN}$, p < 0.001; $N^{\Delta MN}$ versus $\beta\gamma^{\Delta MN}$, p < 0.01; for V-H p < 0.01: control versus $\beta\gamma^{\Delta MN}$ p < 0.01; one-way ANOVA and *post hoc* Tukey's honest significant difference [HSD] test).

(I) Dorso-ventral density plots of H (green, ventral), R/T (red, ventral), and V (blue, dorsal) neurons in control, $N^{\Delta MN}$, and $\beta\gamma^{\Delta MN}$ embryos.

(J) Average dorso-ventral position of H (green, ventral), R/T (red, ventral), and V (blue, dorsal) neurons in control, $N^{\Delta MN}$, and $\beta\gamma^{\Delta MN}$ embryos (mean ± SD; differences significant for V neurons p < 0.001: control versus $N^{\Delta MN}$ and $\beta\gamma^{\Delta MN}$ p < 0.001; for R/T neurons p < 0.001: control versus $N^{\Delta MN}$ and $\beta\gamma^{\Delta MN}$ p < 0.001; for H neurons p < 0.01: control versus $N^{\Delta MN}$ and $\beta\gamma^{\Delta MN}$ p < 0.01; one-way ANOVA and *post hoc* Tukey's HSD test).

For additional data regarding motor neuron organization in $N^{\Delta MN}$ embryos, see Figure S3.
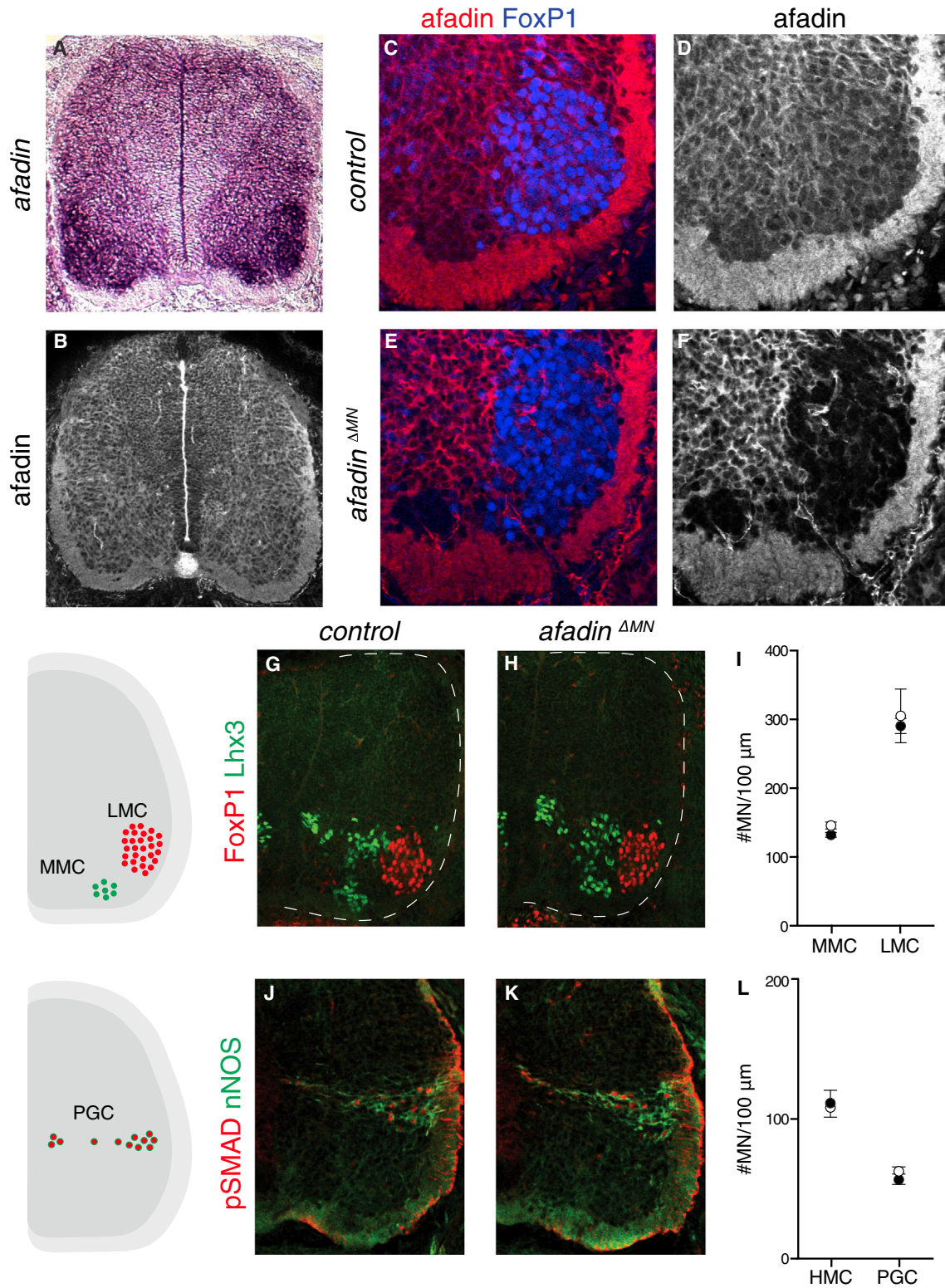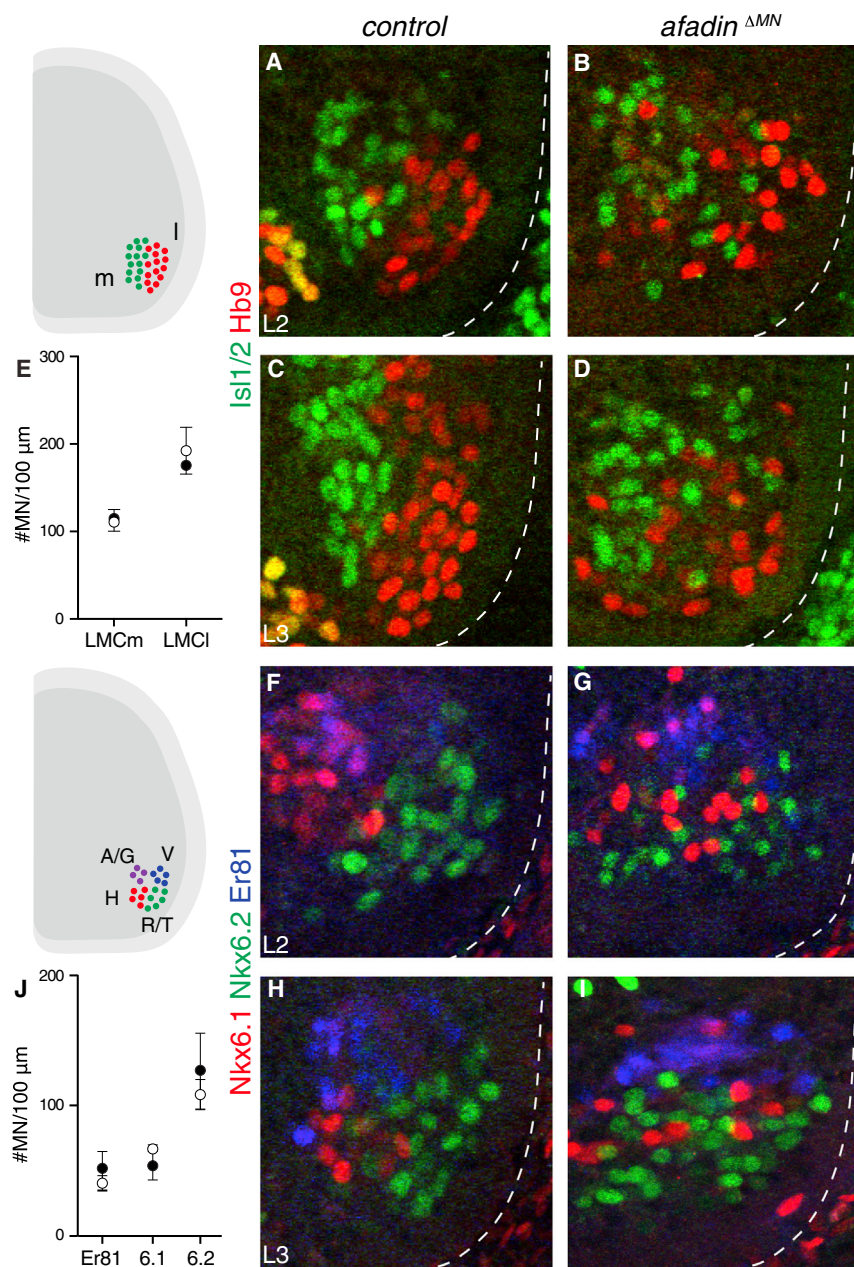
Figure 5. Afadin Expression and Motor Neuron Generation in Developing Spinal Cord

(A and B) Afadin mRNA (A) and protein (B) expression in E13.5 lumbar spinal cord.

(C–F) Afadin expression in E13.5 lumbar spinal cord in control (C and D) and *afadin*$^{\Delta MN}$ (E and F) embryos. FoxP1 identifies LMC neurons.

(G and H) Segregation of Lhx3$^+$ MMC and FoxP1$^+$ LMC neurons in E13.5 lumbar spinal cord of control (G) and *afadin*$^{\Delta MN}$ (H) embryos.

(legend continued on next page)

control   *afadin*$^{\Delta MN}$

Isl1/2 Hb9

A   B

L2

C   D

L3

E

300

#MN/100 μm

200

100

0

LMCm   LMCl

Nkx6.1 Nkx6.2 Er81

F   G

L2

H   I

L3

A/G   V

H

R/T

J

200

#MN/100 μm

100

0

Er81   6.1   6.2

Figure 6. Perturbed Divisional and Pool Organization in Afadin Mutants

(A–D) Isl1/2$^+$ medial and Hb9$^+$ lateral LMC neurons at L2/L3 in E13.5 control (A and C) and *afadin*$^{\Delta MN}$ (B and D) embryos.

(E) Number of LMCm and LMCl neurons in E13.5 lumbar spinal cord of control (C) and *afadin*$^{\Delta MN}$ (●) embryos. Motor neurons/100 μm, mean ± SD.

(F–I) Motor pools at L2/L3 in E13.5 control (F and H) and *afadin*$^{\Delta MN}$ (G and I) embryos. Nkx6.1$^+$, Er81$^+$ adductor/gracilis (A/G) neurons; Er81$^+$, Nkx6.1$^-$ V neurons; Nkx6.2$^+$ R/T neurons; Nkx6.1$^+$, Er81$^-$ H neurons.

(J) Number of Er81$^+$, Nkx6.1$^+$, and Nkx6.2$^+$ motor neurons in E13.5 lumbar spinal cord of control (C) and *afadin*$^{\Delta MN}$ (●) embryos. Motor neurons/100 μm, mean ± SD.

contrast, correlation of LMCl neuron positions of *afadin*$^{\Delta MN}$ and control embryos was reduced (*afadin*$^{\Delta MN}$ versus control LMCl, r = 0.65). Thus, the data indicate that afadin has a specific function in controlling the medio-lateral settling position of LMCl neurons.

Next, we asked whether afadin inactivation has an effect on motor pool organization. Consistent with the divisional data, the pool position analysis indicated that afadin inactivation selectively impairs the ability of motor neurons with a lateral identity (R/T) to settle past motor neurons with a medial identity (H; Figures 7E–7G). In addition, a subtle lateral shift in the position of the H neurons was evident in *afadin*$^{\Delta MN}$ embryos (Figure 7G). However, when we compared the position of H neurons within the divisions, we found that the H pool was still contained within the LMCm area, suggesting that afadin mutant embryos may also present defects in intradivisional medio-lateral pool organization (Figure 7H).

We also analyzed the segregation and clustering of dorsal (V) and ventral (H and R/T) motor pools. Transverse contour density plots indicated that the relative dorso-ventral organization of motor pools is not affected by afadin inactivation (Figures 7I and 7J and S5H). Analyses of dorso-ventral distribution and average position did not reveal significant differences between control and afadin mutants (Figures 7K and 7L and S5F and S5G). As a consequence, the average dorso-ventral distance between pools is not changed

observed a subtle ventral shift in columnar location (Figures S5C and S5E). To provide a quantitative assessment of divisional organization in afadin mutants, we used correlation analysis (Figure S5D). We found that LMCm neuron positions of *afadin*$^{\Delta MN}$ and control embryos were highly correlated (*afadin*$^{\Delta MN}$ versus control LMCm, r = 0.91), indicating that the overall spatial organization of these neurons is not affected by afadin elimination. In

(I) Number of MMC and LMC neurons found in E13.5 lumbar spinal cord of control (C) and *afadin*$^{\Delta MN}$ (●) embryos. Motor neurons/100 μm, mean ± SD.

(J and K) pSMAD$^+$, nNOS$^+$ preganglionic column (PGC) neurons in E13.5 thoracic spinal cord of control (J) and *afadin*$^{\Delta MN}$ (K) embryos.

(L) Number of HMC and PGC neurons in E13.5 thoracic spinal cord of control (C) and *afadin*$^{\Delta MN}$ (●) embryos. Motor neurons/100 μm, mean ± SD.

For additional data regarding afadin and nectin expression in developing spinal cord, see Figure S4.
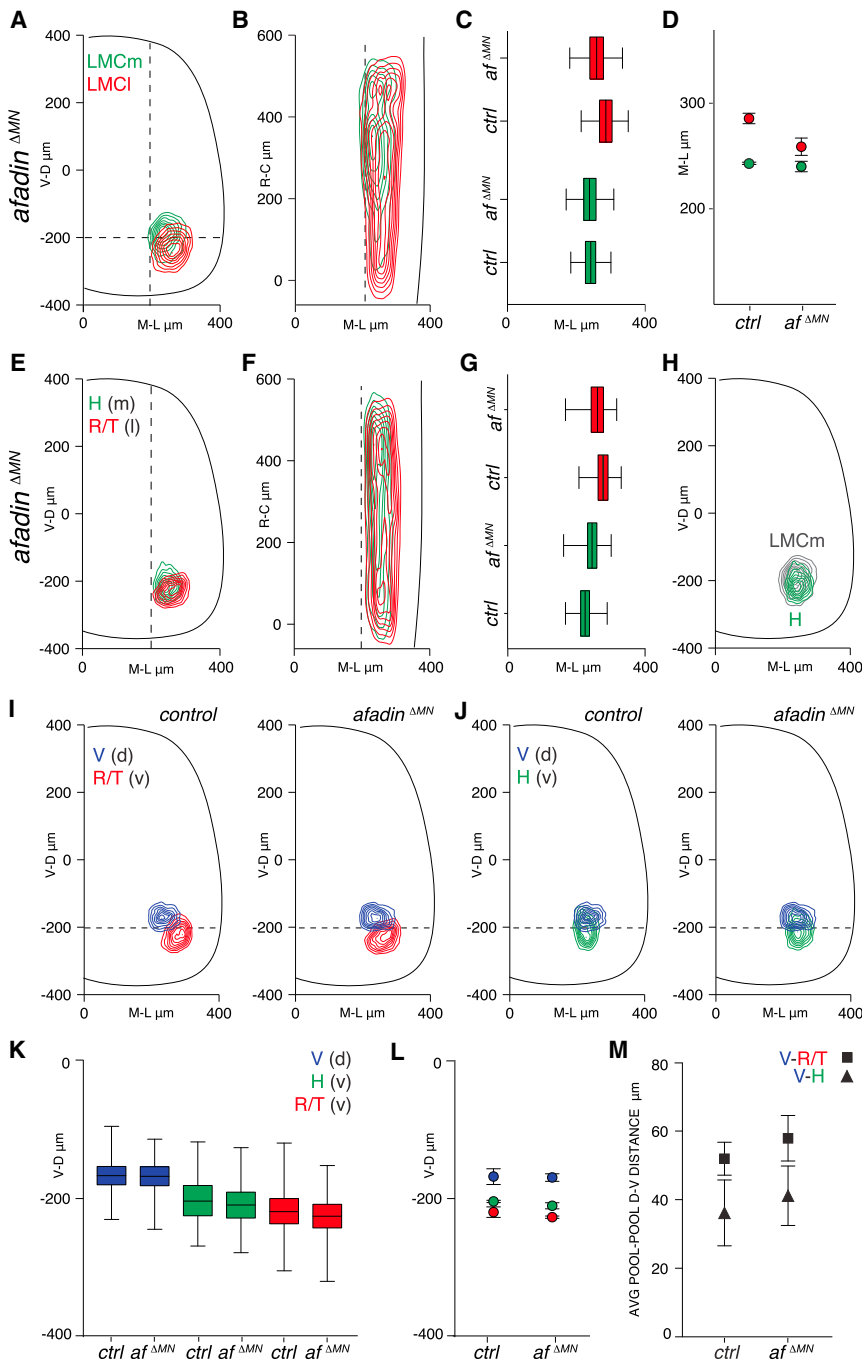
Figure 7. Motor Pool Positioning Defects in Afadin Mutants

(A and B) Transverse (A) and longitudinal (B) contour density plots of LMCm (green) and LMCl (red) neurons in E13.5 *afadin^ΔMN* embryos.

(C) Boxplots showing the distribution of LMCm (green) and LMCl (red) neurons along the medio-lateral axis in control and *afadin^ΔMN* embryos.

(D) Average medio-lateral position of LMCm (green) and LMCl (red) neurons in control and *afadin^ΔMN* embryos (mean ± SD; differences significant for LMCl neurons; t test, p < 0.01).

(E and F) Transverse (E) and longitudinal (F) contour density plots of H (green, medial) and R/T (red, lateral) motor neurons in E13.5 *afadin^ΔMN* embryos.

(G) Boxplots showing the distribution of H (green) and R/T (red) neurons along the medio-lateral axis in control and *afadin^ΔMN* embryos.

(H) Transverse contour density plots of H (green) motor neuron and LMCm (gray) neuron areas in *afadin^ΔMN* and control embryos, respectively.

(I and J) Transverse contour plots of R/T (red, ventral) and V (blue, dorsal) motor neurons (I) and H (green, ventral) and V (blue, dorsal) neurons (J) in control and *afadin^ΔMN* embryos.

(K) Box-plots showing distributions of H (green, ventral), R/T (red, ventral), and V (blue, dorsal) neurons on the dorso-ventral axis in control and *afadin^ΔMN* embryos.

(L) Average dorso-ventral position of H (green), R/T (red), and V (blue) neurons in control and *afadin^ΔMN* embryos (mean ± SD).

(M) Average distance between dorso-ventral positions of V-R/T (■) and V-H (▲) pools in control and *afadin^ΔMN* embryos (mean ± SD).

For additional data regarding motor neuron organization and cadherin/catenin expression and function in *afadin^ΔMN* embryos, see Figures S5 and S6.

tored neurite outgrowth in motor neurons isolated from control and *afadin^ΔMN* embryos grown either on laminin- or N-cadherin-coated dishes. It has been shown previously that motor neurons undergo a 2-fold increase in neurite length and branching when grown on N-cadherin-presenting substrates and that these enhancements are completely abrogated in the absence of catenin function (Demireva et al., 2011). However, we did not observe any significant difference in N-cadherin-

in *afadin^ΔMN* embryos (Figure 7M). These data indicate that afadin signaling specifically controls motor neuron segregation on the medio-lateral axis by regulating LMCl positioning but is not required for motor neuron organization on the dorso-ventral axis.

Next we asked whether afadin is required for cadherin/catenin expression and function. First, we examined the consequences of afadin elimination on the expression of N-cadherin and β-catenin and did not detect any changes in motor neuron area and in motor neuron progenitor zone of *afadin^ΔMN* embryos (Figures S6A–S6L). Second, to test N-cadherin function, we moni-

enhanced neurite outgrowth and branching between control and *afadin^ΔMN* motor neurons (Figures S6M–S6R). Altogether, these experiments indicate that motor neurons do not require afadin activity either for expression of N-cadherin/catenin or for functional interaction with an N-cadherin substrate.

DISCUSSION

The positioning of newly born neurons is a tightly regulated process that is critical for the assembly of the nervous system. In the

spinal cord, nuclear organization of motor neurons into pools is an elaborated morphogenetic feature at the basis of the wiring of spinal sensory motor circuits (Sürmeli et al., 2011; Hinckley et al., 2015; Bikoff et al., 2016). The events controlling motor neuron positioning during development have yet to be clearly defined. Previous studies identified cadherin/catenin adhesive signaling as an important regulator of motor neuron organization but did not provide insights into the molecular and cellular events leading to precise positioning (Price et al., 2002; Demireva et al., 2011). Here, by taking advantage of three-dimensional positional analysis, we uncovered that N-cadherin, via β- and γ-catenin signaling, has a dual role in motor neuron organization. First, it controls columnar dorso-ventral position in the ventral horn. Second, it participates in directing the medio-lateral position of LMCl neurons and divisional segregation. Surprisingly, the data reveal that N-cadherin activity is dispensable for motor pool segregation on the dorso-ventral axis, indicating the existence of other catenin-interacting effectors controlling these events.

In addition, we identified afadin as an important player in motor neuron organization. Afadin elimination has a selective role in the control of LMCl medio-lateral settling, confirming that LMCl neuron inside-out positioning is a key step in controlling motor neuron segregation on the medio-lateral axis and proper layering of divisional subtypes. In contrast, loss of afadin function has no effect on dorso-ventral motor neuron positioning, indicating that nectins do not participate in this aspect of motor pool organization. Altogether, the data support a model where nuclear structure of motor neurons is first initiated by inside-out radial migration, orchestrated by N-cadherin/catenin and afadin activities, controlling the settling of LMCl neurons past LMCm neurons, and is then completed by a second, independent phase that promotes dorso-ventral patterning of motor pools.

Lamination and Nuclear Organization of Spinal Motor Neurons

Precise control of neurogenesis and migration is used during development as a strategy to position neuronal subtypes into specific coordinates. In the developing cortex, inside-out positioning of neurons tightly links neuronal birth date and migratory pattern, controlling the laminar organization of neurons (Hatten, 1999; Marín et al., 2010). Neurons exiting the cell cycle at early time points populate deep cortical layers, whereas neurons generated at later times settle in superficial layers. In contrast, less is known about the mechanisms controlling nuclear organization; however, experimental evidence points to a multi-step process that involves switching between distinct migration modes (Kawauchi et al., 2006; Watanabe and Murakami, 2009; Shi et al., 2017). Limb-innervating motor neurons display prominent nuclear organization and are positioned into discrete clusters, termed pools, that are found at precise coordinates in the spinal cord (Dasen and Jessell, 2009). Previous work indicated that motor neurons migrate radially away from the progenitor zone during development (Leber and Sanes, 1995). Indeed, radial migration is supposed to be at the basis of medio-lateral organization of motor neuron divisions.

Our findings indicate that inactivation of either N-cadherin, β- and γ-catenin, or afadin has a specific effect on the medio-lateral positioning of LMCl neurons, which are found in medial

locations normally occupied by LMCm neurons whose position is unaffected. These data show for the first time that inside-out radial migration is a key step for layering of motor neuron divisions and that N-cadherin/catenin and afadin functions are prominent regulators of this process. Analyses of N-cadherin and β- and γ-catenin mutants revealed an additional role for N-cadherin/catenin signaling in the control of columnar dorso-ventral positioning. However, despite the dramatic ventral shift in LMC neuron location evident in N-cadherin mutants, the relative positioning and segregation of motor pools on the dorso-ventral axis is mostly spared. Altogether, these data imply that other β- and γ-catenin-dependent effectors are in charge of controlling dorso-ventral pool clustering. On the dorso-ventral axis, the positioning and segregation of motor neurons are unaffected by elimination of afadin. Afadin is an essential determinant of nectin function; thus, these data suggest that nectin adhesive recognition is not required for dorso-ventral segregation of motor pools (Takai and Nakanishi, 2003; Takai et al., 2008).

What is regulating motor pool segregation on the dorso-ventral axis? Type II cadherins exhibit complex combinatorial patterns of expression in several areas of the developing nervous system, including motor neurons in the spinal cord, leading to the hypothesis that this family of molecules might be used to generate an adhesive code responsible for controlling cell-cell recognition during development (Suzuki et al., 1997; Redies, 2000; Krishna-K et al., 2011; Hirano and Takeichi, 2012). However, attempts to resolve the contributions of type II cadherins to the control of motor neuron organization have been confounded by the complexity of their expression profiles and adhesive preferences. To date, there is no mouse genetic evidence that elimination of type II cadherins affects motor neuron positioning (Demireva et al., 2011). Recent work in retina and hippocampal circuits suggests that redundancy in heterophilic adhesive recognition of subsets of type II cadherins may mask the contribution of individual members of the family, implying that joint inactivation of selected subsets might be necessary to eliminate their function (Duan et al., 2014; Basu et al., 2017).

Afadin Signaling and Divisional Organization in the Spinal Cord

Our analysis reveals that the events involved in medio-lateral divisional organization closely resemble the ones controlling cortical lamination, suggesting that the same signaling systems may be used in the developing spinal cord. Precise control of cell adhesive interactions is critical for cortical development, regulating the proliferation of neuronal progenitors, stability of the radial glia scaffold, and migration of post-mitotic neurons (Bielas and Gleeson, 2004). The classical cadherin and nectin families of adhesion molecules are key components of the machinery that controls the assembly and maintenance of several types of cell junctions, with catenins and afadin interaction regulating the cross-talk between these molecules (Takai et al., 2008; Hirano and Takeichi, 2012). To date, many members of the cadherin/catenin and nectin/afadin signaling systems have been shown to play important roles during cortical development. Elimination of β-catenin in cortical progenitors results in migratory defects in late-born cortical neurons, and severe cortical lamination phenotypes are also observed in N-cadherin and afadin

mutant mice (Machon et al., 2003; Kadowaki et al., 2007; Gil-Sanz et al., 2014; Yamamoto et al., 2015). Moreover, acute disruption of N-cadherin as well as nectin and afadin functions in cortical neurons perturbs radial migration (Jossin and Cooper 2011; Martinez-Garay et al., 2016). Recent evidence indicates that nectin-based adhesion controls radial migration by acting in concert with reelin and N-cadherin (Gil-Sanz et al., 2013). Interestingly, reelin signaling has also been shown to be involved in spinal motor neuron migration, and, in particular, divisional segregation defects have been observed after perturbation of Reelin-Dab1 signaling (Yip et al., 2003; Palmesino et al., 2010).

Our findings complement and extend these studies, indicating that interplay by cadherin/catenin and nectin/afadin signaling is a conserved developmental mechanism that controls neuronal positioning not only during the assembly of laminar structures, as exemplified in the cortex, but also of nuclear ones. The precise mechanism behind afadin function in motor neurons and its relationship with cadherin/catenin signaling needs to be further addressed. Our data indicate that afadin is not required for N-cadherin/catenin function in motor neurons, suggesting that it might regulate the migration of LMCl neurons by transducing nectin activity. Nectins are not strongly expressed in the spinal cord during development, indicating the possibility that afadin could control migration in a nectin-independent manner (Figures S4C–S4F; Miyata et al., 2009). Altogether, our data support a key role for afadin and catenin adhesive signaling in lamination of motor neuron divisions, highlighting their role as conserved regulators of inside-out migration in the developing nervous system. Thus, it will be interesting in the future to test whether a similar developmental logic and mechanisms are used in the morphogenesis of other spatially ordered structures in the nervous system.

EXPERIMENTAL PROCEDURES

Immunohistochemistry

Embryonic spinal cords were fixed with 4% paraformaldehyde for 90 min, cryoprotected by equilibration with 30% sucrose, frozen in optimum cutting temperature compound (Tissue-Tek), and sectioned using a Leica cryostat. Sections were processed as described previously, and images were acquired on a Zeiss LSM 800 confocal microscope (Demireva et al., 2011).

In Situ Hybridization

In situ hybridization was performed on 16-μm cryostat sections using digoxigenin (DIG)-labeled probes (Demireva et al., 2011). Afadin probes were generated using the following sequences: forward, 5′-CTCTGCAGCTTCAAGCCTT GTTACAAAATTAC-3′; reverse, 5′-GACAGATGTTATCTTAGCTGCTGTTCCA GATG-3′.

Neurite Outgrowth Assay

Motor neurons were dissociated from E10.5 control (*afadin fl/+; olig2::Cre+/−; rosa-lsl-tdTomato fl/+*) or *afadin$^{\Delta MN}$* (*afadin fl/−; olig2::Cre+/−; rosa-lsl-tdTomato fl/+*) embryos and plated on dishes coated with laminin (Sigma) or N-cadherin (R&D Systems). Motor neurons were cultured for 16–20 hr. Neurite length and branching of tdTomato$^+$ neurons were determined using ImageJ (NIH).

Three-Dimensional Analysis of Motor Neuron Subtype Positioning

Motor neuron positions were acquired using the "spots" function of the imaging software Imaris (Bitplane) to assign x and y coordinates. Coordinates were expressed relative to the midpoint of the spinal cord midline, defined as positions x = 0, y = 0. To account for experimental variations in spinal cord size, orientation, and shape, sections were normalized to a standardized spinal

cord whose dimensions where empirically calculated at E13.5 (midline to the lateral edge = 365 μm, midpoint of the midline to the ventral edge = 340 μm). The rostro-caudal coordinates (z axis) were obtained by tracking the order of histological sections. Motor neuron x,y coordinates were accordingly arranged on a z axis consisting of 16 μm bins. We aligned datasets on the z axis by acquiring coordinates starting from the section (z = 0) where either the first Isl1/2$^+$ motor neuron (for divisional analysis) or Nkx6.1$^+$ motor neuron (for pool analysis) appeared and progressed caudally for 512 μm (for a maximum of 33 sections, 16 μm each), covering approximately the rostral half of the lumbar spinal cord. See Table S1 for genotypes, number of embryos, and number of sections per embryo analyzed.

Statistical Analysis

Positional datasets were analyzed using custom scripts in "R project" (R Foundation for Statistical Computing, Vienna, Austria, 2005). For details, see Supplemental Experimental Procedures.

SUPPLEMENTAL INFORMATION

Supplemental Information includes Supplemental Experimental Procedures, six figures, and one table and can be found with this article online at https://doi.org/10.1016/j.celrep.2018.01.059.

AUTHOR CONTRIBUTIONS

C.D., S.P., and N.Z. devised the project, designed experiments, and wrote the manuscript. C.D. and S.P. performed experiments and data analysis. P.H. helped with data analysis. A.A. wrote scripts for analysis in R. T.M.J. provided initial guidance and support for the project.

DECLARATION OF INTERESTS

The authors declare no competing interests.

REFERENCES

Astick, M., Tubby, K., Mubarak, W.M., Guthrie, S., and Price, S.R. (2014). Central Topography of Cranial Motor Nuclei Controlled by Differential Cadherin Expression. Curr. Biol. *24*, 2541–2547.

Basu, R., Duan, X., Taylor, M.R., Martin, E.A., Muralidhar, S., Wang, Y., Gangi-Wellman, L., Das, S.C., Yamagata, M., West, P.J., et al. (2017). Heterophilic Type II Cadherins Are Required for High-Magnitude Synaptic Potentiation in the Hippocampus. Neuron *96*, 160–176.e8.

Beaudoin, G.M., 3rd, Schofield, C.M., Nuwal, T., Zang, K., Ullian, E.M., Huang, B., and Reichardt, L.F. (2012). Afadin, a Ras/Rap effector that controls cadherin function, promotes spine and excitatory synapse density in the hippocampus. J. Neurosci. *32*, 99–110.

Bello, S.M., Millo, H., Rajebhosale, M., and Price, S.R. (2012). Catenin-dependent cadherin function drives divisional segregation of spinal motor neurons. J. Neurosci. *32*, 490–505.

Bielas, S.L., and Gleeson, J.G. (2004). Cytoskeletal-associated proteins in the migration of cortical neurons. J. Neurobiol. 58, 149–159.

Bikoff, J.B., Gabitto, M.I., Rivard, A.F., Drobac, E., Machado, T.A., Miri, A., Brenner-Morton, S., Famojure, E., Diaz, C., Alvarez, F.J., et al. (2016). Spinal Inhibitory Interneuron Diversity Delineates Variant Motor Microcircuits. Cell 165, 207–219.

Dasen, J.S., and Jessell, T.M. (2009). Hox networks and the origins of motor neuron diversity. Curr. Top. Dev. Biol. 88, 169–200.

Dasen, J.S., De Camilli, A., Wang, B., Tucker, P.W., and Jessell, T.M. (2008). Hox repertoires for motor neuron diversity and connectivity gated by a single accessory factor, FoxP1. Cell 134, 304–316.

De Marco Garcia, N.V., and Jessell, T.M. (2008). Early motor neuron pool identity and muscle nerve trajectory defined by postmitotic restrictions in Nkx6.1 activity. Neuron 57, 217–231.

Demireva, E.Y., Shapiro, L.S., Jessell, T.M., and Zampieri, N. (2011). Motor neuron position and topographic order imposed by β- and γ-catenin activities. Cell 147, 641–652.

Dessaud, E., Yang, L.L., Hill, K., Cox, B., Ulloa, F., Ribeiro, A., Mynett, A., Novitch, B.G., and Briscoe, J. (2007). Interpretation of the sonic hedgehog morphogen gradient by a temporal adaptation mechanism. Nature 450, 717–720.

Duan, X., Krishnaswamy, A., De la Huerta, I., and Sanes, J.R. (2014). Type II cadherins guide assembly of a direction-selective retinal circuit. Cell 158, 793–807.

Gil-Sanz, C., Franco, S.J., Martinez-Garay, I., Espinosa, A., Harkins-Perry, S., and Müller, U. (2013). Cajal-Retzius cells instruct neuronal migration by coincidence signaling between secreted and contact-dependent guidance cues. Neuron 79, 461–477.

Gil-Sanz, C., Landeira, B., Ramos, C., Costa, M.R., and Müller, U. (2014). Proliferative defects and formation of a double cortex in mice lacking Mltt4 and Cdh2 in the dorsal telencephalon. J. Neurosci. 34, 10475–10487.

Harris, T.J.C., and Tepass, U. (2010). Adherens junctions: from molecules to morphogenesis. Nat. Rev. Mol. Cell Biol. 11, 502–514.

Hatten, M.E. (1999). Central nervous system neuronal migration. Annu. Rev. Neurosci. 22, 511–539.

Hinckley, C.A., Alaynick, W.A., Gallarda, B.W., Hayashi, M., Hilde, K.L., Driscoll, S.P., Dekker, J.D., Tucker, H.O., Sharpee, T.O., and Pfaff, S.L. (2015). Spinal Locomotor Circuits Develop Using Hierarchical Rules Based on Motorneuron Position and Identity. Neuron 87, 1008–1021.

Hirano, S., and Takeichi, M. (2012). Cadherins in brain morphogenesis and wiring. Physiol. Rev. 92, 597–634.

Hollyday, M., and Hamburger, V. (1977). An autoradiographic study of the formation of the lateral motor column in the chick embryo. Brain Res. 132, 197–208.

Ikeda, W., Nakanishi, H., Miyoshi, J., Mandai, K., Ishizaki, H., Tanaka, M., Togawa, A., Takahashi, K., Nishioka, H., Yoshida, H., et al. (1999). Afadin: A key molecule essential for structural organization of cell-cell junctions of polarized epithelia during embryogenesis. J. Cell Biol. 146, 1117–1132.

Jossin, Y., and Cooper, J.A. (2011). Reelin, Rap1 and N-cadherin orient the migration of multipolar neurons in the developing neocortex. Nat. Neurosci. 14, 697–703.

Kadowaki, M., Nakamura, S., Machon, O., Krauss, S., Radice, G.L., and Takeichi, M. (2007). N-cadherin mediates cortical organization in the mouse brain. Dev. Biol. 304, 22–33.

Kawauchi, D., Taniguchi, H., Watanabe, H., Saito, T., and Murakami, F. (2006). Direct visualization of nucleogenesis by precerebellar neurons: involvement of ventricle-directed, radial fibre-associated migration. Development 133, 1113–1123.

Krishna-K, K., Hertel, N., and Redies, C. (2011). Cadherin expression in the somatosensory cortex: evidence for a combinatorial molecular code at the single-cell level. Neuroscience 175, 37–48.

Landmesser, L.T. (2001). The acquisition of motoneuron subtype identity and motor circuit formation. Int. J. Dev. Neurosci. 19, 175–182.

Leber, S.M., and Sanes, J.R. (1995). Migratory paths of neurons and glia in the embryonic chick spinal cord. J. Neurosci. 15, 1236–1248.

Leone, D.P., Srinivasan, K., Chen, B., Alcamo, E., and McConnell, S.K. (2008). The determination of projection neuron identity in the developing cerebral cortex. Curr. Opin. Neurobiol. 18, 28–35.

Lin, J.H., Saito, T., Anderson, D.J., Lance-Jones, C., Jessell, T.M., and Arber, S. (1998). Functionally related motor neuron pool and muscle sensory afferent subtypes defined by coordinate ETS gene expression. Cell 95, 393–407.

Machon, O., van den Bout, C.J., Backman, M., Kemler, R., and Krauss, S. (2003). Role of β-catenin in the developing cortical and hippocampal neuroepithelium. Neuroscience 122, 129–143.

Mandai, K., Nakanishi, H., Satoh, A., Obaishi, H., Wada, M., Nishioka, H., Itoh, M., Mizoguchi, A., Aoki, T., Fujimoto, T., et al. (1997). Afadin: A novel actin filament-binding protein with one PDZ domain localized at cadherin-based cell-to-cell adherens junction. J. Cell Biol. 139, 517–528.

Marín, O., Valiente, M., Ge, X., and Tsai, L.H. (2010). Guiding neuronal cell migrations. Cold Spring Harb. Perspect. Biol. 2, a001834.

Martinez-Garay, I., Gil-Sanz, C., Franco, S.J., Espinosa, A., Molnár, Z., and Mueller, U. (2016). Cadherin 2/4 signaling via PTP1B and catenins is crucial for nucleokinesis during radial neuronal migration in the neocortex. Development 143, 2121–2134.

McHanwell, S., and Biscoe, T.J. (1981). The sizes of motoneurons supplying hindlimb muscles in the mouse. Proc. R. Soc. Lond. B Biol. Sci. 213, 201–216.

Miyata, M., Ogita, H., Komura, H., Nakata, S., Okamoto, R., Ozaki, M., Majima, T., Matsuzawa, N., Kawano, S., Minami, A., et al. (2009). Localization of nectin-free afadin at the leading edge and its involvement in directional cell movement induced by platelet-derived growth factor. J. Cell Sci. 122, 4319–4329.

Miyata, M., Maruo, T., Kaito, A., Wang, S., Yamamoto, H., Fujiwara, T., Mizoguchi, A., Mandai, K., and Takai, Y. (2017). Roles of afadin in the formation of the cellular architecture of the mouse hippocampus and dentate gyrus. Mol. Cell. Neurosci. 79, 34–44.

Oishi, K., Nakagawa, N., Tachikawa, K., Sasaki, S., Aramaki, M., Hirano, S., Yamamoto, N., Yoshimura, Y., and Nakajima, K. (2016). Identity of neocortical layer 4 neurons is specified through correct positioning into the cortex. eLife 5, 1–26.

Palmesino, E., Rousso, D.L., Kao, T.-J., Klar, A., Laufer, E., Uemura, O., Okamoto, H., Novitch, B.G., and Kania, A. (2010). Foxp1 and lhx1 coordinate motor neuron migration with axon trajectory choice by gating Reelin signalling. PLoS Biol. 8, e1000446.

Price, S.R., De Marco Garcia, N.V., Ranscht, B., and Jessell, T.M. (2002). Regulation of motor neuron pool sorting by differential expression of type II cadherins. Cell 109, 205–216.

Rakic, P. (1974). Neurons in rhesus monkey visual cortex: systematic relation between time of origin and eventual disposition. Science 183, 425–427.

Ramon y Cajal, S. (1894). La fine structure des centres nerveux. Proc. R. Soc. Lond. 55, 444–468.

Redies, C. (2000). Cadherins in the central nervous system. Prog. Neurobiol. 61, 611–648.

Romanes, G.J. (1964). The motor pools of the spinal cord. Prog. Brain Res. 11, 93–119.

Shi, W., Xianyu, A., Han, Z., Tang, X., Li, Z., Zhong, H., Mao, T., Huang, K., and Shi, S.-H. (2017). Ontogenetic establishment of order-specific nuclear organization in the mammalian thalamus. Nat. Neurosci. 20, 516–528.

Sockanathan, S., and Jessell, T.M. (1998). Motor neuron-derived retinoid signaling specifies the subtype identity of spinal motor neurons. Cell 94, 503–514.

Stepien, A.E., Tripodi, M., and Arber, S. (2010). Monosynaptic rabies virus reveals premotor network organization and synaptic specificity of cholinergic partition cells. Neuron 68, 456–472.

Sürmeli, G., Akay, T., Ippolito, G.C., Tucker, P.W., and Jessell, T.M. (2011). Patterns of spinal sensory-motor connectivity prescribed by a dorsoventral positional template. Cell *147*, 653–665.

Suzuki, S.C., Inoue, T., Kimura, Y., Tanaka, T., and Takeichi, M. (1997). Neuronal circuits are subdivided by differential expression of type-II classic cadherins in postnatal mouse brains. Mol. Cell. Neurosci. *9*, 433–447.

Takai, Y., and Nakanishi, H. (2003). Nectin and afadin: novel organizers of intercellular junctions. J. Cell Sci. *116*, 17–27.

Takai, Y., Ikeda, W., Ogita, H., and Rikitake, Y. (2008). The immunoglobulin-like cell adhesion molecule nectin and its associated protein afadin. Annu. Rev. Cell Dev. Biol. *24*, 309–342.

Vanderhorst, V.G., and Holstege, G. (1997). Organization of lumbosacral motoneuronal cell groups innervating hindlimb, pelvic floor, and axial muscles in the cat. J. Comp. Neurol. *382*, 46–76.

Watanabe, H., and Murakami, F. (2009). Real time analysis of pontine neurons during initial stages of nucleogenesis. Neurosci. Res. *64*, 20–29.

Yamamoto, H., Maruo, T., Majima, T., Ishizaki, H., Tanaka-Okamoto, M., Miyoshi, J., Mandai, K., and Takai, Y. (2013). Genetic deletion of afadin causes hydrocephalus by destruction of adherens junctions in radial glial and ependymal cells in the midbrain. PLoS ONE *8*, e80356.

Yamamoto, H., Mandai, K., Konno, D., Maruo, T., Matsuzaki, F., and Takai, Y. (2015). Impairment of radial glial scaffold-dependent neuronal migration and formation of double cortex by genetic ablation of afadin. Brain Res. *1620*, 139–152.

Yip, Y.P., Capriotti, C., and Yip, J.W. (2003). Migratory pathway of sympathetic preganglionic neurons in normal and reeler mutant mice. J. Comp. Neurol. *460*, 94–105.